

STUDY OF WELDABILITY OF HIGH STRENGTH LOW ALLOY STEELS WITH BORON AT LASER WELDING*

Jefferson Lisboa Lelis¹
Maiara Rodrigues Gouveia²
Marcos Roberto Soares da Silva³

Abstract

Nowadays, due the development of new hot rolled strips at USIMINAS, established the necessity of realizing studies to define new parameters for the welding machine of new pickling line, in order to improve mechanical and metallurgical properties of these materials. The aim of this study was to evaluate the weldability of high strength low-alloy steel with low boron content with tensile strength above 600MPa. The influence of energy input and preheating temperature on the mechanical properties of hot rolled strips were analyzed at three distinct thickness (2, 4 and 6 mm). To perform these evaluations were used tensile test, micro-hardness, metallography (micro and macro examination) and scanning electron microscopy analysis. In resume, a good welding performance was achieved, increasing preheating temperature and the welding energy higher than 60%.

Keywords: Laser welding; Weldability; Low-alloy steel; carbon-boron steel.

¹ Metallurgical Engineer, Specialist in Welding Engineering, MBA in Business Management and Development, Hot Rolling Production Engineer, Usiminas, Cubatão, São Paulo - Brazil.

² Metallurgical Engineer, Cold Rolling Production Engineer, Usiminas, Cubatão, São Paulo - Brazil.

³ Metallurgical Engineer, Technical Support Rolling Manager, Usiminas, Cubatão, São Paulo-Brazil.

1 INTRODUCTION

In the last years, due to the search for better productivity and quality in the welding process in steel mill continuous production lines, it was justified investments in laser welding machines. Owing to the high energy density, the laser welding process has a very narrow heat-affected area and excellent quality welding [1]. Even with all the benefits this process provides, there are still challenges in certain types of materials and dimensions. High strength coiled hot-rolled strip are being developed for automotive applications constantly and require a match in the welding parameters when compared to the most common steels (materials without alloying elements such as Niobium, Titanium, Vanadium and Boron). Another factor that has an impact on this welding process is the welding difficulty with thicknesses higher than 6 mm (depending on the laser power capacity and other specifications of the welding machine).

An experiment was carried out in the laser welding machine implanted at USIMINAS pickling line, in order to evaluate the influences of welding parameters in carbon-boron steel such as thickness, welding speed, energy input and preheating power. The aim of this paper is to evaluate better results of mechanical properties in order to avoid process stoppages due to weld ruptures.

2 MATERIAL AND METHOD

The study material is a high strength low-alloy steel with low boron (SAE 15B30 or carbon-boron steel) having a carbon equivalent of 0.60. The laser welding machine used has a CO₂ laser with a maximum power capacity of 12 kW.

2.1 Welding Parameters

According to tables 1, 2 and 3, the values of the welding parameters (energy input and preheating power) were determined for

each thickness (2.0, 4.0 and 6.0 mm). The power of the laser remained constant at 11.7 kW for all the experiment welds, so the variation of the energy input was through the change of the welding speed.

Table 1: Welding parameters to thickness 2.0mm.

Sample	Parameters		
	Welding Speed	Preheating Power	Energy Input
	m/min	kW	J/cm
E2V45PA20	5.3	7	1267
E2V45PA35	5.3	14	1267
E2V45PA50	5.3	19	1267
E2V55PA20	6.4	8	1036
E2V55PA35	6.4	14	1036
E2V55PA50	6.4	19	1036
E2V65PA20	7.7	7	785
E2V65PA35	7.7	13	785
E2V65PA50	7.7	19	785

Table 2: Welding parameters to thickness 4.0mm.

Sample	Parameters		
	Welding Speed	Preheating Power	Energy Input
	m/min	kW	J/cm
E4V30PA30	3.5	11	1900
E4V30PA45	3.5	18	1900
E4V30PA60	3.5	23	1900
E4V40PA30	4.7	11	1425
E4V40PA45	4.7	18	1425
E4V40PA60	4.7	23	1425
E4V50PA30	5.9	11	1140
E4V50PA45	5.9	17	1140
E4V50PA60	5.9	24	1140

Table 3: Welding parameters to thickness 6.0mm.

Sample	Parameters		
	Welding Speed	Preheating Power	Energy Input
	m/min	kW	J/cm
E6V20PA45	2.5	17	2714
E6V20PA60	2.5	23	2714
E6V20PA75	2.5	29	2714
E6V30PA45	3.5	17	1900
E6V30PA60	3.5	23	1900
E6V30PA75	3.5	30	1900
E6V40PA45	4.7	17	1425
E6V40PA60	4.7	24	1425
E6V40PA75	4.7	29	1425

Label:

Sample identification **EXVYPAZ** where:
EX = thickness sample;
VY = Welding speed (% of 12,5 m/min)
PAZ = Preheating power (% of 40 kW).

2.2 Mechanical and metallographic tests

For this study, were evaluated tensile test, microhardness test, macrographic and micrograph analyzes, as well as a detailed analysis in scanning electron microscope (SEM) [2-5].

3 RESULTS AND DISCUSSION**3.1 Influences of the welding parameters in the tensile test**

The tensile test was performed on all samples described above and the results of tensile strength (TS), yield strength (YS) and elongation (e) obtained are shown in the graphs of figure 1. Figures 1.a and 1.b show that for thicknesses of 2.0 mm and 4.0 mm all tensile test ruptures were in the base metal and maintained uniformity in the result. The figure 1.c shows E6V40PA60 sample that broke in the weld zone due thickness of 6mm and low energy input (1425 J/cm). For the same thickness, samples welded with low speed and was possible achieve higher energy input (1900 and 2714 J/cm). In those cases weld rupture did not occur, reaching results of yield strength, elongation and base metal resistance similar to the average.

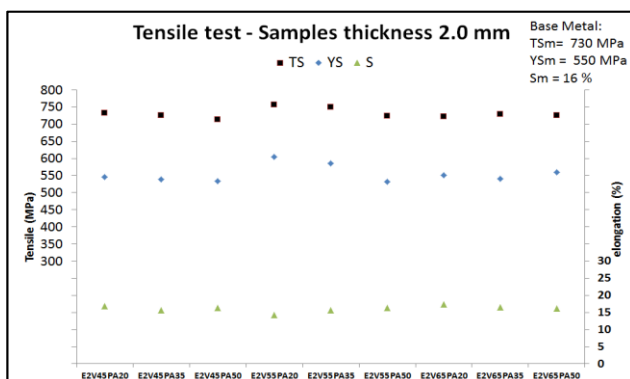


Figure 1.a Tensile test – (thickness 2.0mm).

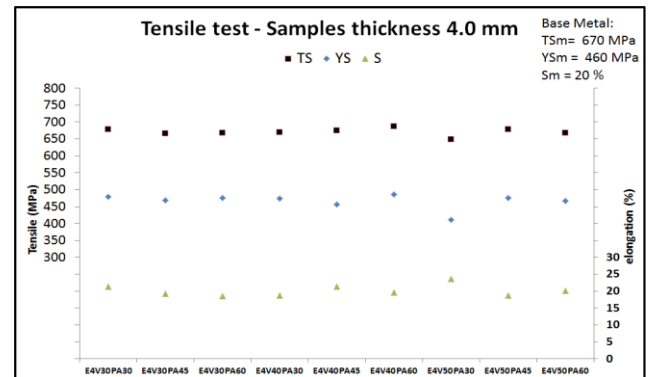


Figure 1.b Tensile test – (thickness 4.0mm).

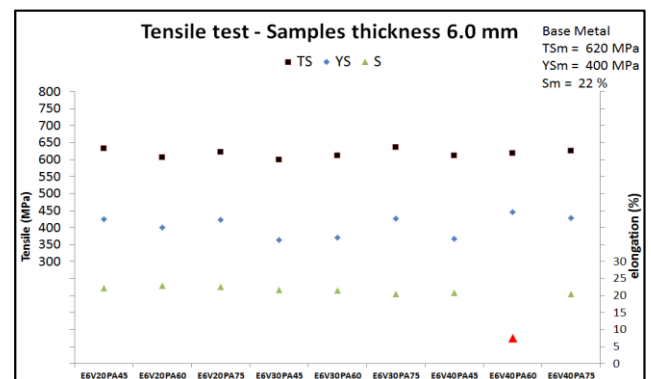


Figure 1.c Tensile test – (thickness 6.0mm).

3.2 Influences of the welding parameters in the microhardness test

With the results obtained in the tensile test, specific samples were chosen for the microhardness test, in order to identify potential contributors for the occurrence of weld rupture in the E6V40PA60 sample. Samples with 6mm of thickness were defined with three different levels of energy input, being 2714, 1900 and 1425 J/cm. The samples E6V20PA45, E6V30PA45 and E6V40PA60 are shown in figure 2. The test was made on both sides, being one in the transition zone (TZ), three in the heat affected zone (HAZ) and two in the fusion zone (FZ).

The profiles found in figure 2 obtained similar behaviors of Vickers microhardness but with different intensities. The base metal (BM) represents the microhardness of the material studied, then a small addition in the TZ (between BM and HAZ), points of higher hardness in the HAZ (cooling with high rates obtain to a

microstructure with higher hardness) and a drop in the FZ.

It is observed in graphs of figure 2.a that Vickers microhardness values for the sample with the highest energy input (2714 J/cm) obtained values lower than 400 HV in the HAZ (according to Mei [6] values of Vickers hardness near to 250/300 HV is critical for crack susceptibility) but as the material has high equivalent carbon (≈ 0.60), in the welding process it is more difficult the control of inhibiting the formation of martensitic structures with high hardness value [7]. As the energy input decreases, the welding speeds increase and this situation becomes more critical and is possible to verify higher Vickers microhardness values. With energy input of 1900 J/cm in sample E6V30PA45 (figure 2.b), higher Vickers microhardness values are already observed at 500 HV. Finally, the sample E6V40PA60, where the rupture was in the weld and not in the base metal, with a welding speed of 4.8 m/min and energy input of 1425 J/cm, the Vickers microhardness values reached close to 600 HV in the HAZ, becoming very susceptible to cracking and high residual stresses in its microstructure.

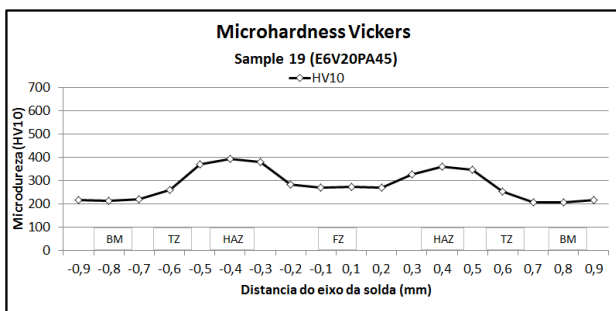


Figure 2.a Microhardness sample E6V20PA45.

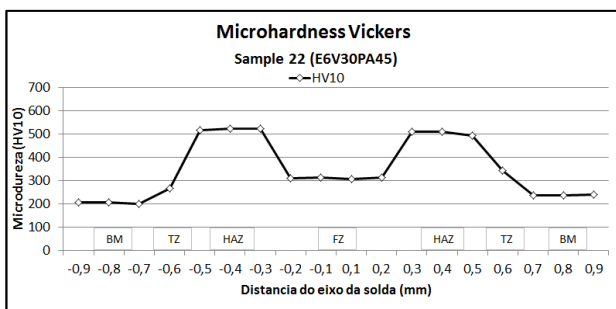


Figure 2.b Microhardness sample E6V30PA45.

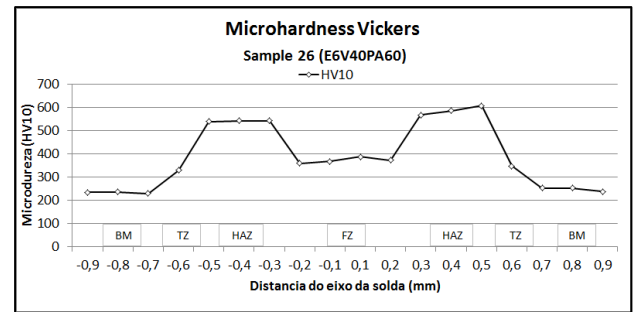


Figure 2.c Microhardness sample E6V40PA60.

3.3 Influences of the welding parameters in the metallographic analyzes.

In order to correlate the results obtained with microscopic analysis, the same samples were used (E6V20PA45, E6V30PA45 and E6V40PA45).

3.3.1 Macroscopic welding aspect

In figure 3, comparing the zone affected by heat, we can see that the width of this region affected by heat is heterogeneous along the depth. This behavior is demonstrated with greater intensity in samples with lower energy input.

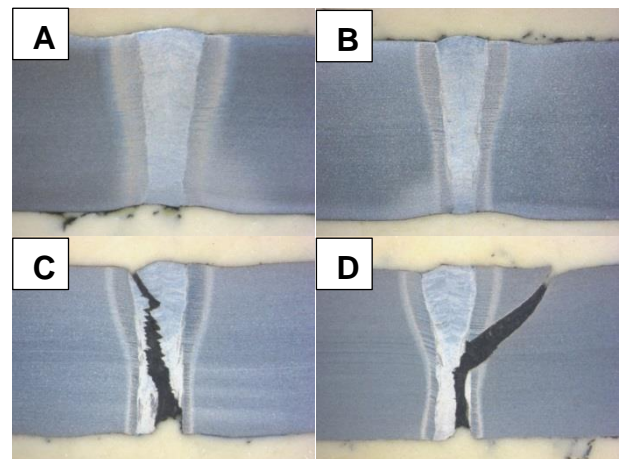


Figure 3 Macrograph - magnification 50x

- (A) E6V20PA45 (E=2714 J/cm)
- (B) E6V30PA45 (E=1900 J/cm)
- (C) E6V40PA45 (E=1425 J/cm)
- (D) E6V40PA45 (E=1425 J/cm)

This heterogeneity may not be beneficial to transition zone because it causes distinct stress buildup in adjacent regions of weld and higher cooling rates near the melt line.

3.3.2 Microscopic welding aspect

In figure 4 and 5 there are some representative sample micrographs with different energy input. In figure 4, HAZ and FZ didn't reveal any discontinuity, and has a more homogeneous transition between base metal and HAZ. With lower energy input, the result was opposite and cracks in HAZ and FZ of this sample were found (figure 5).

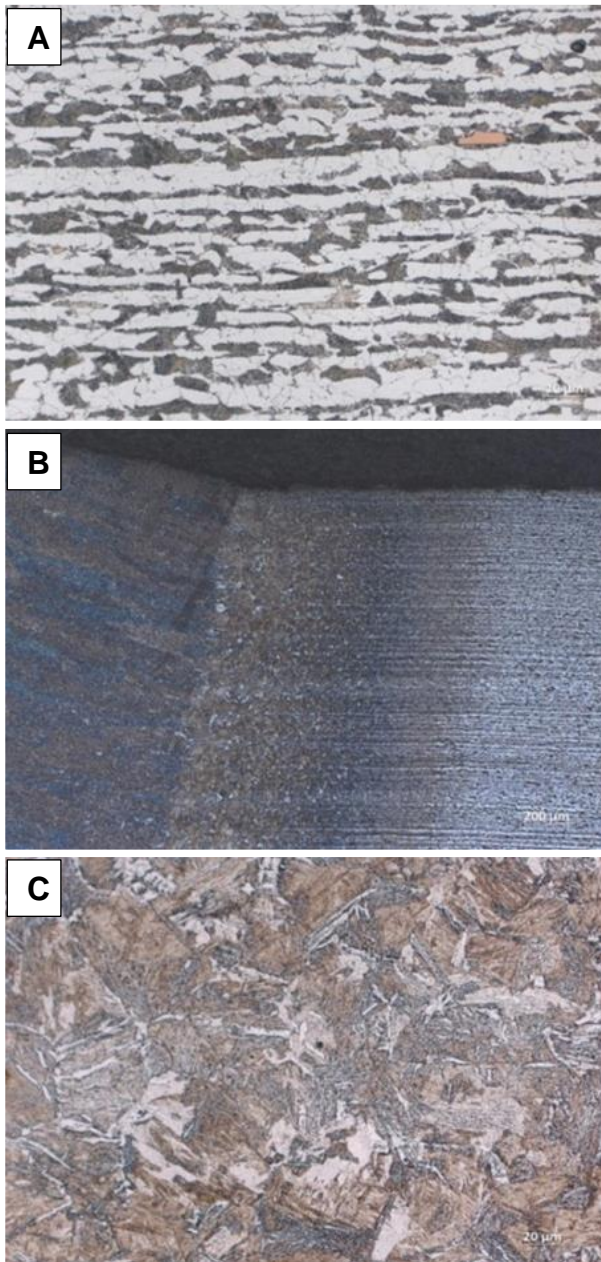


Figure 4 micrograph sample E6V20PA45
 (A) BM (pearlite + ferrite) - magnification 500X
 (B) BM + HAZ + FZ - magnification 50X
 (C) HAZ (martensite) - magnification 500X

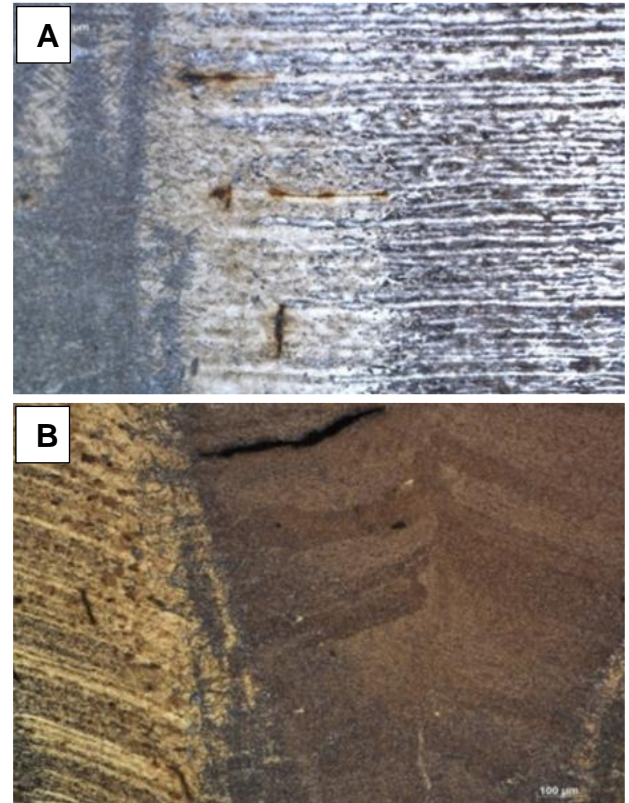


Figure 5 micrograph sample E6V20PA45
 (A) HAZ crack - magnification 100X
 (B) HAZ + FZ crack - magnification 100X

3.4 Microscopic aspect of the crack and fracture region using scanning electron microscope (SEM)

To investigate in detail the root cause of the crack presented in the previous section, it was analyzed in the Scanning Electron Microscope (SEM), in order to confirm the inference of hot crack.

It is observed that in figure 6 and 7 the aspect around the fracture surface shows micro cavities, while inside a gross melt structure, confirming that it is a solidification crack. This type of crack occurs when the strand contains films of low melting phase, which persist in the liquid state between solidified grains. Some residual chemical elements inherent in the steelmaking process, such as sulfur and phosphorus, reduce remaining liquid solidification point between interdendritic grain boundaries, being unable to accommodate the increasing deformations by contraction.

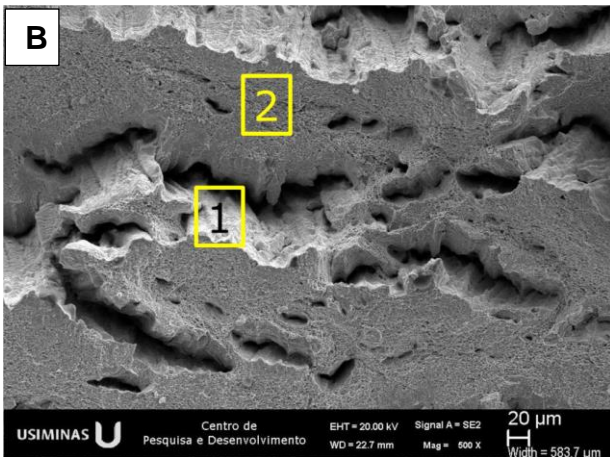
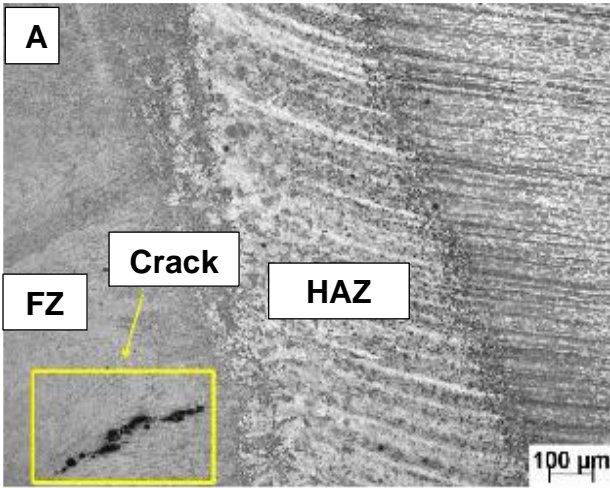


Figure 6 General appearance of the hot crack found on fracture surface - E6V40PA60 sample
 (A) SEM – magnification 100x
 (B) SEM – magnification 500x

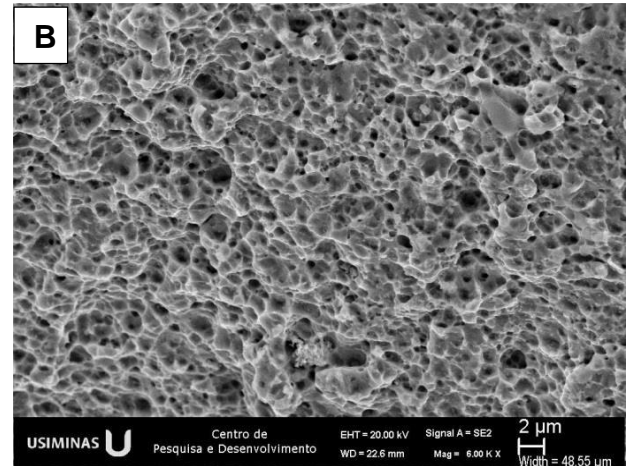
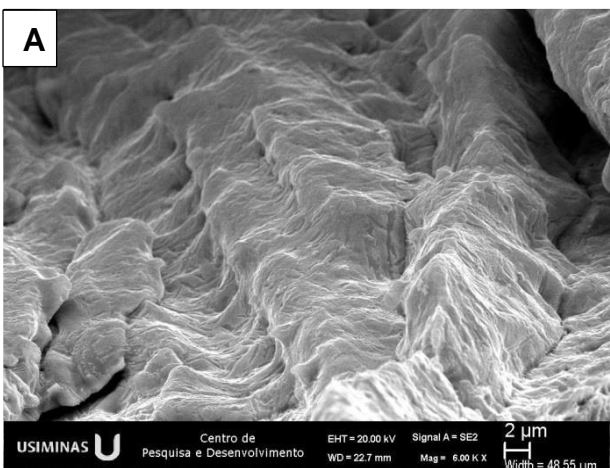


Figure 7 Crack detail found on fracture surface - E6V40PA60 sample – magnification 6000x
 (A) Detail inside of crack (region 1)
 (B) Detail outside of crack (region 2)

SEM analyzes by EDS (energy dispersive X-ray spectroscopy) revealed high counting intensity for carbon and iron elements and, with less intensity, for phosphorus, aluminum, silicon and manganese, as shown in figure 8.

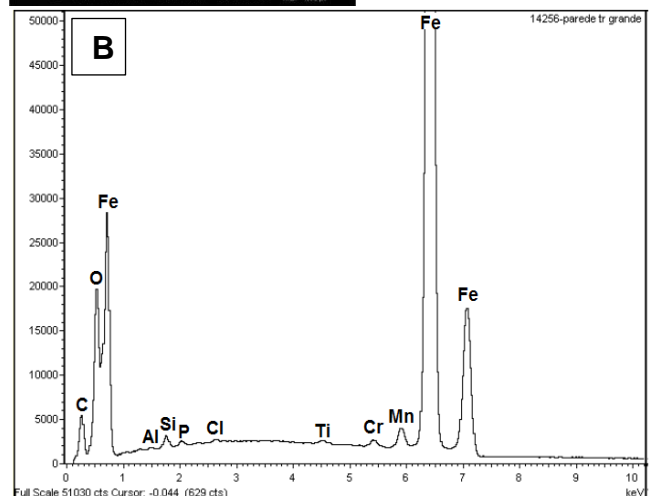
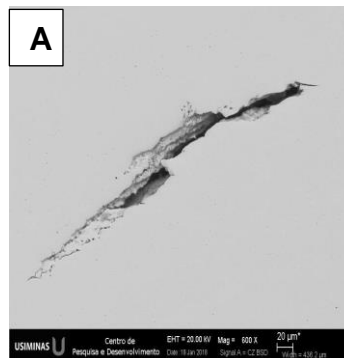


Figure 8 Crack analysis result by SEM/EDS
 (A) Magnification 600x
 (B) Typical EDS obtained within the crack.

It was also evaluated by scanning electron microscopy (SEM) the general aspect of the fracture surface (sample E6V40PA60) and it's observed that there is a lack of fusion at root weld. Figure 9 perfectly illustrates the smooth appearance in the region of the root solder, confirming that no melting material occurred in that particular region.

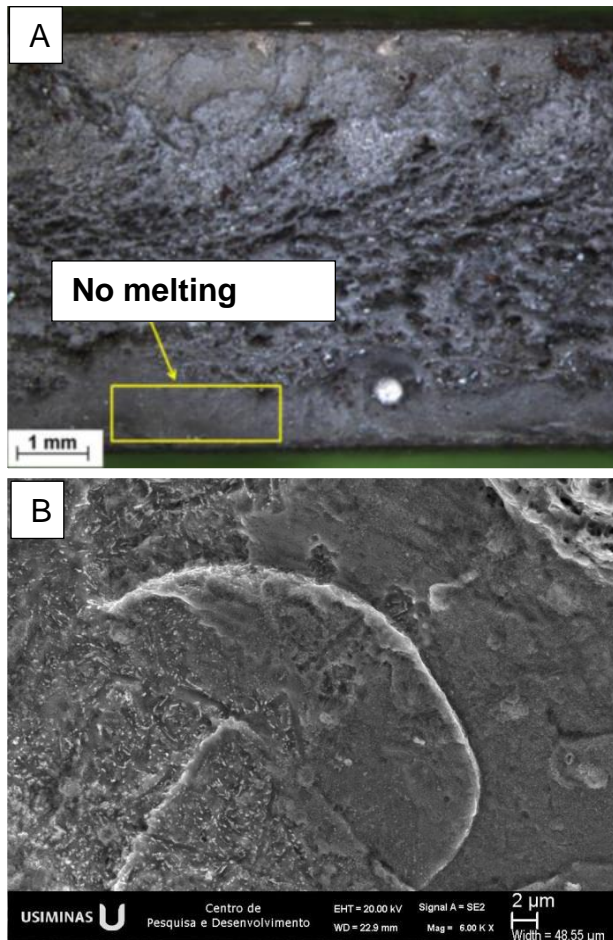


Figure 9 Fracture surface aspects by SEM - sample E6V40PA60

- (A) General appearance of the fracture surface
(B) Detail of the region with no melting.

4 CONCLUSION

The results show that, for carbon-boron steel, autogen laser welding showed better performance in welded sample with higher energy input. In the tensile test occurred weld rupture in one sample analyzed, which had a thickness of 6 mm and a lower energy input (1425 J/cm). This sample

showed, in an optical microscopy analysis, hot cracks in the zone affected by the heat (HAZ) and melt zone (FZ). With more detailed, it was analysis the crack region in the Scanning Electron Microscope (SEM) that showed an aspect of fracture from solidification crack. This hot crack was evidenced that it had influence with the high rates of cooling in the process of solidification of the fusion well.

Another point evaluated was the microhardness profiles. While sample of thickness 6 mm with energy input of 2714 J/cm obtained a microhardness profile with maximum range of 200 HV, sample with energy input of 1425 J/cm obtained results with 400 HV and in HAZ region with 600 HV.

Therefore, the alteration of the energy input parameters and the preheating to higher levels, according to each studied thickness, brought greater guarantee for the process and allowed the welding of these materials on industrial scale. In this way, we can conclude in this study that for thicknesses of 6.0mm the best combination of welding parameters to have a better homogeneity of the weld and base metal is using energy input of 2714 J / cm avoiding high cooling rates.

Acknowledgments

The pickling line team of Usiminas that helped in study feasibility and the University of São Paulo for technical support. Especially Douglas Souza, Alexandre Alves and Gabriela Miranda from Usiminas laboratory and Israel Martins from technical support.

REFERENCES

- ¹ LIMA, M. S. F; Lasers in Material Processing. In: LACKNER, Lasers in Chemistry: Influencing matter. 2008. p.1195-1209
- ² ASTM A370-17. Standard Test Methods and Definitions for Mechanical Testing of Steel Products. ed. 2017
- ³ ABNT. NBR 6673. Produtos Planos de Aço – Determinação das propriedades mecânicas a tração. ed.1981.
- ⁴ DIN EN ISO 6892-1. Metallic Materials – Tensile Testing – Part 1: Method of test at room temperature. ed. 2017
- ⁵ ASTM A370-17. Standard Test Method for Microindentation Hardness of Materials. ed. 2017
- ⁶ MEI, P. R.; SILVA, A. L. C.. Aços e ligas especiais. 3. ed. Sumaré: Eletrometal S.A. Metais Especiais, 2006.
- ⁷ MODENESI, P. J.; Fluxo de calor em soldagem, Universidade Federal de Minas Gerais, 2003